Contrasting juxtaposition of two paradigms for diazotrophy in an Earth System Model of intermediate complexity

Ulrike Löptien[1,2] and Heiner Dietze[1,2]

[1]GEOMAR Helmholtz Centre for Ocean Research Kiel, Düsternbrooker Weg 20 24105 Kiel, Germany
[2]Institute for Geosciences, University of Kiel, Ludewig-Meyn-Str. 10, 24118 Kiel, Germany

Correspondence: Ulrike Löptien (uloeptien@geomar.de)

Abstract. Nitrogen fixers, or diazotrophs, play a key role in the carbon and nitrogen cycle of the world oceans, but the controlling mechanisms are not comprehensively understood yet. The present study compares two paradigms on the ecological niche of diazotrophs in an Earth System Model (ESM). In our standard model configuration, which is representative for most of the state-of-the-art pelagic ecosystem models, diazotrophs take advantage of zooplankton featuring a lower food preference for

5 diazotrophs than for ordinary phytoplankton. We compare this paradigm with the idea that diazotrophs are more competitive under oligotrophic conditions, characterized by low (dissolved, particulate, organic and inorganic) phosphorous availability. Both paradigms are supported by observational evidence and lead to a similar good agreement to the most recent and advanced observation-based nitrogen fixation estimate in our ESM framework. Further, we illustrate that the similarity between the two paradigms breaks in a RCP 8.5 anthropogenic emission scenario. We conclude that a more advanced understanding of the

10 ecological niche of diazotrophs is mandatory for assessing the cycling of essential nutrients, especially under changing environmental conditions. Our results call for more *in-situ* measurements of cyanobacteria biomass if major controls of nitrogen fixation in the oceans are to be dissected.

1 Introduction

Nitrogen is an essential element in the metabolism of plants. Even though it is much more abundant in air than for example

15 carbon dioxide, the assimilation of carbon by phytoplankton in vast regions of the ocean is considered to be limited by the availability of nitrogen. Among the reasons for this is that most phytoplankton cannot use the molecular nitrogen, that is so abundant in air, because it cannot break the exceptionally strong chemical bond between the two nitrogen atoms constituting molecular nitrogen (N_2). An exception to this rule are so-called nitrogen fixing microorganisms (bacteria and archaea) that are capable of breaking this bond and thus can utilize the molecular nitrogen of the air. Their total input of bioavailable

20 nitrogen to the ocean is substantial: current estimates range from 70 to 200 $TgNyr^{-1}$ (c.f., Großkopf et al., 2012; Gruber and Sarmiento, 1997; Tang et al., 2019b; Wang et al., 2019). Paleo-records suggest that for the last several thousand years, this input has been balanced by denitrification and anaerobic ammonium oxidation (anammox) which converts bioavailable forms of N (e.g. NO_3^-, NO_2^-) under low-oxygen conditions back to N_2 (Altabet et al., 2012). The apparent balance of sources and sinks of bioavailable N suggests a coupling mechanism between these sources and sinks. Such coupling mechanisms and

25 related controls on the overall oceanic N-budget are discussed controversially (e.g., Gruber, 2016; Wang et al., 2019) - also because the controls on nitrogen fixation are not comprehensively understood.

There is, however, consensus, that anthropogenic forcing, such as global warming and input of bioavailable nitrogen to the ocean, modulates the turnover of bioavailable nitrogen in the ocean which might have far-reaching consequences (Duce et al., 2008; Krishnamurthy et al., 2007; Krishnamurthy. et al., 2009; McMahon et al., 2015). Some studies suspect that N_2-
30 fixation might increase regionally in the future, adding extra nutrients to already-overfertilized systems (e.g., Tang et al., 2019; Wasmund et al., 2001), or even result in vicious cycles (e.g., Vahtera et al., 2007). This comprehension has triggered efforts to capture the respective dynamics in numerical models which explicitly resolve oceanic transport mechanisms (such as currents and mixing) along with the turnover of biogeochemical species (nutrients, carbon and oxygen) - with the aim to forecast the effects of changing environmental conditions and thereby facilitating management and mitigation measures.

35 A generic approach to capture the major aspects of the marine N-cycle in numerical models is to include an explicit representation of diazotrophs as an extra functional group, that is distinctly different to the representation of ordinary non-fixing phytoplankton (e.g., Fennel et al., 2001; Moore et al., 2001; Paulsen et al., 2017). The underlying model assumptions and respective mathematical formulations vary from one model to another, but they typically agree on (1) diazotrophs are capable of utilizing N_2, while ordinary phytoplankton is not and (2) diazotrophs grow slower (or at least not faster) than ordinary phyto-
40 plankton, because of the metabolic cost involved in providing means to break the strong bond between the two nitrogen atoms constituting N_2. When taken alone, a direct deduction of these two assumptions is that diazotrophs only have an advantage over ordinary phytoplankton in regions where bioavailable nitrogen supply is below the demands of ordinary phytoplankton, relative to the phosphorus supply (Deutsch et al., 2007; Schmittner et al., 2008). In the remainder of the ocean, ordinary phytoplankton would suppress the relatively slow growing diazotrophs by competing more successfully for resources, such as bioavailable
45 phosphorus (P), iron (for which diazotrophs have a higher demand) and light (e.g., Falcón et al., 2005; LaRoche and Breitbarth, 2005; Mills and Arrigo, 2005). Observations, however, indicate no such correlation between nitrogen fixation and a nutrient supply that is low in nitrogen relative to, e.g., bioavailable phosphate (Capone et al., 2005; Gruber, 2004). Further perplexity is added by the fact that diazotrophs are known to increase their internal N:P ratios via fixation beyond the needs of ordinary phytoplankton. Thereby they ultimately overstock the system with extra nitrogen - which would downsize the extent of their
50 very own ecological niche (c.f., Landolfi et al., 2013).

All prognostic models we have reviewed so far, include some additional assumptions that give diazotrophs an additional competitive advantage, that outweighs their tendency to change their environmental conditions to their disadvantage (by adding extra nitrogen to the system). These additional assumptions are not always explicitly formulated, but are often imposed during trial and error exercises where model parameters are tuned in an attempt to get a good fit to observations. One assumption often
55 implicitly incorporated (but rarely explicitly mentioned) is *selective grazing* by zooplankton, where ordinary phytoplankton is exposed to higher grazing pressure than the (slower-growing) diazotrophs (e.g., Keller et al., 2012; Paulsen et al., 2017). This paradigm may be founded on the fact that some diazotrophs can produce toxins that fend off grazers (Hawser et al., 1992). An alternative paradigm, equally consistent with observational studies (e.g., Degerholm et al., 2006), has been suggested recently by Pahlow et al. (2013) who use an optimality based model to illustrate, that oligotrophy - especially in P, can favour

60   diazotrophy. The idea is that diazotrophs outcompete ordinary phytoplankton under P-depleted conditions because they can allocate more P to intracellular P-uptake machinery. The underlying physiological explanation is that diazotrophs presumably need less P to build their N-uptake machinery, which is already taken care of by the nitrogen-fixation machinery (which is known not to need so much P). Flavors of this paradigm, *low P-demands* of diazotrophs, have been explored in the literature already (Mulholland et al., 2002; Landolfi et al., 2015). In the present study, we add to the ongoing discussion by comparing

65   the implications of the *selective grazing* with the *low P-demands* paradigm. A major focus is on future projections, carried out with the UVic 2.9 Earth System Model (Weaver et al., 2001). The major aim is to illustrate the far reaching implications of both paradigms in a generic model that is currently used to project into our warming future and to assess geoengineering options (see, e.g., Keller et al., 2014; Kemena et al., 2019; Mengis et al., 2016; Reith et al., 2016). Our experiments are designed to constrain the envelope of model responses as set by each of the paradigms. We find (and illustrate in this study) that the

70   development of a reliable model must be preceded by additional in-situ observations.

2   Methods

In the following, we describe the Keller et al. (2012) reference model (Sect. 2.1) and two flavors of this reference model (Sect. 2.2), representative of the *selective grazing* and *low P-demands* paradigm, respectively. Sect. 2.3 describes the numerical experiments and Sect. 2.4 the considered observations.

75   ## 2.1   The Reference Model

We use the UVic 2.9 Earth System Model, documented and extensively assessed in Keller et al. (2012). We refer to this standard model version since it is extensively used (e.g., Keller et al., 2014; Kemena et al., 2019; Reith et al., 2016), well documented (Keller et al., 2012; Schmittner et al., 2008) and was used earlier to study diazotrophy (e.g., Landolfi et al. (2017); Somes and Oschlies (2015)). The model is of intermediate complexity and thus allows for running a multitude of simulations

80   to quasi-equilibrium. The horizontal resolution is $1.8°$ in latitude and $3.6°$ in longitude in all submodules (ocean, including biogeochemistry, dynamic-thermodynamic sea ice module, atmospheric energy-moisture balance model, land module, with an active terrestrial vegetation component, and simple land ice). The ocean submodule is based on a three-dimensional primitive-equation model (Pacanowski, 1995). The vertical discretization of the ocean comprises 19 levels and increases gradually from $50\,m$ at the surface to $500\,m$ at depth. The vertical background mixing parameter, κ_h, is $0.15\,cm^2 s^{-1}$ throughout the water

85   column. In the Southern Ocean (south of $40°$S) this background value, κ_h, is increased by $1.0\,cm^2 s^{-1}$. An anisotropic viscosity scheme, suggested by Large et al. (2001), is implemented to improve the equatorial circulation (Somes et al., 2010). A marine pelagic biogeochemical model is coupled to the ocean circulation component. Its prognostic variables are ordinary (i.e. non-diazotrophic) phytoplankton (P_o), diazotrophic phytoplankton (P_d), zooplankton (Z), detritus (D), nitrate (NO_3), phosphate (PO_4), dissolved oxygen (O_2), dissolved inorganic carbon (DIN) and alkalinity (ALK). The model is described in detail in

90   Keller et al. (2012) and Schmittner et al. (2008). Note that the dispersive numerics of the oceanic advection occasionally

produces small negative values in phytoplankton and zooplankton concentrations. These values are set to zero in the model evaluation.

In the following, we present a choice of details relevant for the simulated dynamics of diazotrophs (relevant model parameters are listed in Tab.1): phytoplankton growth is generally controlled by the availability of light and nutrients (here, nitrate, phosphate and iron, where the latter is parameterized rather than explicitly resolved). Phytoplankton blooms are terminated by zooplankton grazing, once the essential nutrients are depleted and the related reduction in phytoplankton growth does not longer keep up with the grazing pressure, that has built up during the bloom. For ordinary phytoplankton the maximum potential growth rate is

$$J_o^{max} = a \cdot \left(\frac{Fe}{k_{Fe} + Fe} \right) exp(T/15.65), \tag{1}$$

where k_{Fe}=0.1 $mmol\,Fe/m^3$ is the *half-saturation constant* for iron (Fe)-limitation and $a = 0.6\,d^{-1}$ determines the maximum potential growth rate at an ambient temperature $T = 0°C$.

For diazotrophs the formulation of the maximum potential growth is similar, but diazotrophs are disadvantaged in nitrate-replete waters by $C_d = 0.4$. In addition, growth is stalled in waters colder than $15°C$:

$$J_D^{max} = C_d \cdot a \cdot max \left(0, \frac{Fe}{k_{Fe} + Fe} \right) \cdot exp((T/T_b) - 2.6). \tag{2}$$

The actual growth rate of non-diazotrophic phytoplankton, J_O, is, in case of low irradiance (I) and/or nutrient depleted conditions, the maximum potential rate J_o^{max} reduced by the following implementation of Liebig's law of the minimum:

$$J_O = min \left(J_{IO}, J_O^{max} \frac{NO_3}{k_N + NO_3}, J_O^{max} \frac{PO_4}{k_P + PO_4} \right), \tag{3}$$

where k_N and k_P are the *half saturation constants* for NO_3 and PO_4, respectively.

The actual growth rate of diazotrophs, J_D, is similar but it is not affected by nitrate deficiency:

$$J_D = min \left(J_{ID}, J_D^{max} \frac{PO_4}{k_P^d + PO_4} \right), \tag{4}$$

The light-limited growth J_{IO} and J_{ID} are both determined by:

$$J_{IOandD} = \frac{\alpha I J_{OandD}^{max}}{(\alpha I)^2 + (J_{OandD}^{max})^2}. \tag{5}$$

The initial slope of the P-I curve (α) is set to 0.1 $(W/m^2)^{-1}d^{-1}$. Diazotrophs take up available nitrogen following:

$$NO3_{upt} = min \left(J_{ID}, \frac{min(NO_3, PO_4 \cdot 16)}{(k_P^d \cdot 16) + min(NO_3, PO_4 \cdot 16)} \cdot J_D^{max} \right) \cdot P_D, \tag{6}$$

where P_D denotes the biomass of diazotrophs (in units $molN/m^3$). When no or not enough bioavailable N is available, nitrogen fixation tops the respective N pool up to a Redfield-ratio of N:P=16. Note that the above formulation differs slightly from the original formulation of Keller et al. (2012) which reads:

$$NO3_{upt} = min \left(J_{ID}, \frac{PO_4}{k_P^d + PO_4} \cdot J_D^{max} \right) \cdot \frac{NO_3}{(k_P^d \cdot 16) + NO_3} \cdot P_D, \tag{7}$$

Our minor change ensures a more realistic behavior where no nitrogen is fixed under nitrate-replete conditions. When applied to the reference model version, the difference to the original Keller et al. (2012) simulation turned out to be negligible.

The reference version of Keller et al. (2012) is an implementation of the preferential grazing paradigm. Grazing is determined by:

$$Graze = \mu_{max} \cdot Z \cdot \theta \cdot P, \qquad (8)$$

with a maximum growth rate μ_{max} = 0.4 d^{-1}. Grazing on ordinary phytoplankton, P_O, is calculated by setting $\theta = \theta_o = 0.3$. Grazing on diazotrophs, P_D, is calculated with a lower grazing preference $\theta = \theta_d = 0.1$.

2.2 Implementation of the two Paradigms

We integrate two sets of numerical model configurations. The first set explores the paradigm *selective grazing*, represented by the model setup GRAZ and assumes that diazotrophs are grazed less than ordinary phytoplankton. The second set explores the paradigm *low P-demands*, represented by the model setup OLIGO. We consider both paradigms individually to constrain the envelope of model responses as set by each of the paradigms. To ensure comparability between the paradigms we identify parameters for both paradigms which represent available observations in an "optimal" way (see below). Finally we compare the respective "optimal" representatives of the two paradigms, OLIGO and GRAZ, in Section 3.

The *selective grazing* paradigm is implemented by adjusting the grazing preferences for diazotrophs and ordinary phyto-plankton, θ_d and θ_o, with the additional constraint $\theta_d + \theta_o = 0.4$. In addition, C_d is varied in attempt to minimize the misfit to observations. In total, we explored 24 combinations of the parameters θ_d, θ_o and C_d. In the following, GRAZ refers to the most realistic member of the set of 24 that outperforms the reference version of Keller et al. (2012) (c.f., Tab. 1). The respective model assessment metric is based on the most recent estimate for global nitrogen fixation, provided by Wang et al. (2019). More specifically we calculate the sum of absolute deviations between the locally estimated nitrogen fixation of Wang et al. (2019) and our simulated nitrogen fixation (mean absolute error):

$$cost = \left| \left(\frac{1}{N_m} \sum_{j=1}^{N_m} (a_j - \hat{a}_j) \right) \right|. \qquad (9)$$

N_m denotes the number of estimated values for nitrogen fixation (on the model grid), a_j stands for an 'observation' at location j and $\hat{a}_j$ for the corresponding model result. We consider climatological annual means. Note that this choice of misfit metrics inevitably adds a subjective element and the respective choice will impact the results of the optimization procedure (see Löptien and Dietze, 2015, 2017). A choice has to be made, however, and here we follow a standard approach (c.f., Pontius et al., 2008; Sauerland et al., 2018; Willmott and Matsuura, 2005). Note that solutions with very low biomass of diazotrophs (below an integrated value of 10 TgC) are not considered.

The second paradigm, represented by OLIGO, assumes that diazotrophs can cope better with oligotrophic conditions than ordinary phytoplankton. This paradigm is implemented by (1) setting equal grazing preferences for diazotrophs and ordinary phytoplankton conforming with the additional constraint of $\theta_d + \theta_o = 0.4$ and (2) tuning the half-saturation constant for phosphate limitation of diazotrophs k_P^d (where the values considered are smaller than the original value). Again, C_d is varied in addition to minimize the misfit to observations. In total we explore 24 values for k_P^d and C_d. The respective parameter ranges

are listed in Tab.1. In the following OLIGO refers to the most realistic member of the set of 24 that, according to the metric defined in Equation 9, outperforms the reference version of Keller et al. (2012) (c.f., Tab. 1). Please note that in terms of misfit
145 to observed climatologies of phosphate, nitrate and oxygen REF, GRAZ and OLIGO perform comparable to one another: when considering the World Ocean Atlas 2005 (Garacia et al., 2006), all respective differences in the (volume weighted) root mean squared errors of the three model versions are smaller than the corresponding average (volume weighted) standard deviations of the observations.

2.3 Numerical Experiments

150 The two sets of tuning experiments start from the equilibrated state of what is dubbed *reference run* in Getzlaff and Dietze (2013) and are integrated for 2000 model years with constant, pre-industrial CO_2 emissions. Respective experiment evaluations (as carried out with Equation 9) refer to the average of the last 10 years of these simulations, hindcasting historic conditions. In addition, we will show results from simulations of GRAZ and OLIGO, covering the period 1800-2150. They start with the historical state and are continued with the CO_2 emission scenario RCP 8.5 (Riahi et al., 2011).

155 ### 2.4 Observational Data

In situ observations of diazotrophic biomass and nitrogen fixation rates, such as compiled by Luo et al. (2012), are very useful but still too sparse to allow for robust comparisons between model and observations. This has been a serious drawback hindering the identification of the major controls of diazotrophy. This study exploits the most recent and most comprehensive product from Wang et al. (2019), that fills data gaps by combining observations with inverse biogeochemical and prognostic
160 ocean modelling - an approach pioneered by Deutsch et al. (2007).

3 Results

Our tuning exercises for the two paradigms *selective grazing* and *low P-demands* identified two respective "best" simulations out of two sets of 24 model integrations, which, according to Equation 9, feature the highest similarity to the most recent estimate of global oceanic nitrogen fixation (setups GRAZ and OLIGO; c.f., Sect.2.2). In the following, we present the respec-
165 tive model results with respect to diazotrophy under historic climate conditions. These results are put into perspective to the reference model version REF. We continue with the results from RCP 8.5 scenario integrations.

Both "best" representatives of the two considered paradigms, GRAZ and OLIGO, feature a very similar fit to the observational estimate for nitrogen fixation, clearly superior to the reference simulation REF (the respective costs are 18.2 and 17.6, versus 27.7 $mmol\ N/m^2/yr$). A comparison of our simulations with the, unfortunately very sparse, but independent (in the
170 sense that this data has not been used to identify our the "best" simulations with Equation 9) data collection of diazotrophic biomass from Luo et al. (2012), indicates that the simulated distribution of diazotrophs based on OLIGO is more realistic than in GRAZ. The biomass of diazotrophs in GRAZ is apparently too low. When taking the upper 10% percentiles as a measure for bloom intensities (derived from the respective histograms of positive local annual mean values), OLIGO lies with 716

$mg\ C/m^2$ much closer to the observations (598 $mg\ C/m^2$) than GRAZ (282 $mg\ C/m^2$) and REF (320 $mg\ C/m^2$). Please

175   note, however, that the model data are climatological while the observations are rather anecdotal such that the comparison

relies on the implicit assumption that, e.g., seasonal variations are small (also assumed by, e.g., Landolfi et al., 2015).

    Figure 1 and 2 give a visual impression of the above listed numerical estimates for the goodness of fit. The reference

simulation features too sharp spatial gradients in nitrogen fixation, when compared to the estimate of Wang et al. (2019)

(Fig.1a and d). Particular high values for the simulated fixation in REF occur in the tropical Pacific at the edge of the upwelling

180   regions and in the Indian Ocean, while the observational estimate shows a more homogenous pattern in east-west direction.

Consistent with the fact that OLIGO and GRAZ are tuned against this estimate, the spatial pattern in the simulated amount

of fixed nitrogen in both these simulations are smoother when compared to REF and the maximum values roughly match the

observational estimate.

    Even though OLIGO and GRAZ are very similar, some smaller differences among the two are evident: while GRAZ features

185   generally rather low fixation rates in the Southern Hemisphere, this model version seems most realistic in the North Atlantic.

With respect to diazotroph biomass, the differences between the setups are more pronounced. While the simulated pattern in

nitrogen fixation roughly matches the distribution of diazotrophs in REF (Fig.1a, compared to Fig.2a) and GRAZ (Fig.1b,

compared to Fig.2b), this relation is not as evident for OLIGO: e.g., the amount of fixed nitrogen in the western tropical Pacific

is rather low compared to abundance of diazotrophs (Fig.1c, compared to Fig.2c). The major reason why the overall pattern

190   in dizotroph abundance and fixation do not fully match in OLIGO is that diazotrohs find an ecological niche in oligotrophic

regions (as they require less P than ordinary phytoplankton) without the need to fix atmospheric nitrogen. As desert dwellers

they occupy more area but, even so, they can not necessarily sustain high production rates since access to essential bioavailable

phosphorous is limited. Correspondingly, the quota of annual mean fixation rates versus the biomass of diazotrophs is in

OLIGO more than 3 smaller than in REF and factor 2 smaller than in GRAZ. Also, in contrast to REF and GRAZ, minimum

195   values even go down to zero for OLIGO. Note that these quotas were based on locations with a diazotrophic biomass of more

than 5 mgC/m^2 only (to avoid division by very small numbers).

    In a next step, we determine the parameter sensitivities for the two paradigms, *selective grazing* and *low P-demands* (which

optimal solutions are represented by GRAZ and OLIGO, resp.). Specifically, we explore the sensitivity of changes in the half

saturation constant, k_P^d, versus changes in the food preference, θ_d (based on the respective ensembles of simulations described

200   in Sect.2.2, while C_d is kept constant on the respective optimal level). Changing both parameters, θ_d and k_P^d, by 20% of their

covered range (0.02 and 0.0088, resp.) leads on average to a much larger change in the amount of fixed nitrogen for the *se-*

lective grazing paradigm, compared to *low P-demands* (16.8 and 0.8 $Tg\ N\ yr^{-1}$, respectively). For the integrated biomass

of diazotrophs however, the respective changes are similar for both paradigms (4.9 $Tg\ C$ for *selective grazing* v.s. 5.8 $Tg\ C$

for *low P-demands*). Note, in this context that for both paradigms, the biomass of diazotrophs reacts strongly nonlinear to

205   parametric changes. Interestingly, decreasing the food preference for diazotrophs can even lead to a *tipping point* where the

spatial distribution of diazotrophs is shifted entirely to the upwelling regions.

We conclude that the paradigm *low P-demands* produces a model behavior that is much more robust towards parameter changes than the *selective grazing* paradigm, in the sense that small changes in (rather unconstrained) model parameters effect

210 moderate changes in the quality of the fit to observations. In contrast, small changes to the *selective grazing* paradigm might even induce a regime shift.

A question which arises in this context, is whether the relatively large parameter sensitivity of the paradigm *selective grazing* is also reflected in the model sensitivities towards environmental changes. To explore the effects of changing climate conditions, we projected the model versions OLIGO and GRAZ into a warming future, corresponding to the RCP 8.5 emission scenario.

215 The response of both, OLIGO and GRAZ, are closely tied to an increasing vertical stratification effected by an ocean, that is warmed from above. The water expands at the surface and this increases the vertical density gradient, such that the energy requirements for vertical mixing are increased, because mixing is now associated with pushing lighter, more buoyant water downwards. The increased energy demands for mixing result in a dampening of mixing events and, overall, in less nutrients mixed upwards to the sun-lit surface. Among the processes setting in are (1) a reduction of phosphate supply to the surface

220 (globally and in oligotrophic regions), (2) an increase of oligotrophic regions where phosphate concentrations are depleted at the surface. Such an increase in the size of the oligotrophic regions is captured well in both model versions: following Polovina et al. (2008) we define oligotrophic regions as regions featuring a chlorophyll *a* concentration of less than $0.07 \ mg Chl a m^{-3}$ at the surface. Based on this threshold and applying a constant conversion factor of $1.59 \ mg Chl a mmol N^{-1}$, we find that oligotrophic regions expand by 92% and 90% from 2000 to 2100 for OLIGO and GRAZ, respectively - both of which are in

225 the same order of magnitude as the 1998 to 2006 satellite based estimate of Polovina et al. (2008) (19% per decade).

Because of their underlying paradigm, OLIGO and GRAZ respond very differently to this increase in oligotrophic regions - even though they share a very similar behavior under historical conditions: in the simulation OLIGO, the diazotrophs can take advantage of the increasing vertical stratification because the diazotrophs are expertly exploiting oligotrophic conditions. The black line in Fig.3a shows that the biomass of diazotrophs increases globally along with an increase in size of the oligotrophic

230 regions. In addition, Fig.3b illustrates that, even though the size of oligotrophic regions and the diazotrophic biomass increases, the nitrogen fixation decreases in OLIGO. The reason is a reduced total supply of phosphorous to the surface in (expanded) oligotrophic regions which, in our model, puts an upper limit on nitrogen fixation. Additionally, nitrogen fixers have in the extended oligothrophic regions a competitive advantage over ordinary phytoplankton, because they require less P for their subsistence. Subsistence is, however, not necessarily correlated with high production rates which, ultimately, are limited by the

235 availability of phosphorous - whose limitation provided the niche for diazotrophs in OLIGO.

In contrast, the development of nitrogen fixation and abundance of diazotrophs goes much more hand-in-hand in GRAZ and the projected evolution of both variables differs strongly from OLIGO: an initial increase in both variables is followed by a subsequent decay. Such switching behavior at arbitrary tipping points (that are set by the model parameters) are typical for the rather generic zooplankton formulation used here and have been described, e.g., in Löptien and Dietze (2017), their Sect.3.2.

240 Note, however, that for both model versions the Bay of Bengal features a sudden pronounced onset of nitrogen fixation in the mid 2000s, which is visible even in the global mean. We anticipate that this abrupt change might be to a particularly pronounced sea surface temperature increase in this region.

Biogeosciences
Discussions

4 Conclusions

We have been exploring two paradigms that are proposed in the literature to essentially define the environmental conditions
245 or niches where oceanic diazotrophs may thrive - even though they typically grow slower than ordinary phytoplankton, with
which they compete for essential resources such as phosphate. The first paradigm, a de-facto standard in global earth system
modelling, builds on selective grazing, where the diazotrophs are exposed to a grazing pressure that is reduced relative to
other, ordinary phytoplankton. The second paradigm, based on more recent considerations, assumes that diazotrophs have
lower (dissolved, particulate, organic and inorganic) phosphorous demands than other phytoplankton. Our experiments with
250 an Earth System Model of intermediate complexity show that both paradigms are apparently equally consistent with the most
recent and elaborate estimate of global oceanic nitrogen fixation, which combines observations with prognostic modelling and
data-assimilation techniques (Wang et al., 2019). Our experiments also show that the similarity of the model versions based
on the differing paradigms breaks in projections into a warming future. This suggests that current observational data are not
sufficient to constrain the sensitivity of the dynamics of bioavailable nitrogen under changing environmental conditions. We
255 find that for assessing the fidelity of respective paradigm additional observations of diazotrophic biomass are needed most. To
this end, the quota of nitrogen fixation versus the respective biomass of diazotrophs may prove especially helpful.

Data availability. The model output is preliminary archived at https://nextcloud.ifg.uni-kiel.de/index.php/s/iYx7CWaGN8rx8KE and will
be provided in the Institute repository after review. The observational data collected by Luo et al. (2012) are available via
https://doi.pangaea.de/10.1594/PANGAEA.774851 and cited in the references.

260 *Author contributions.* Both authors were involved in the design of the work, in data analysis, in data interpretation and in drafting the article.

Competing interests. The authors declare that they have no conflict of interest.

References

Altabet, M.A., Higginson, M.J. and Murray, D.W.: The effect of millennial-scale changes in Arabian Sea denitrification on atmospheric CO_2, Nature, 415,159-162. https://doi.org/10.1038/415159a, 2002.

270 Capone, D. G., Burns, J. A., Montoya, J. P., Subramaniam, A., Mahaffey, C., Gunderson, T., Michaels, A.F., and Carpenter, E.J. : Nitrogen fixation by Trichodesmium spp.: an important source of new nitrogen to the tropical and subtropical North Atlantic Ocean. Global Biogeochem. Cycles, 19, GB2024. https://doi.org/10.1029/2004GB002331, 2005.

Degerholm, J., Gundersen, K., Bergman, B., and Söderbäck, E.: Phosphorus-limited growth dynamics in two Baltic Sea cyanobacteria, Nodularia sp. and Aphanizomenon sp., FEMS Microbiology Ecology, 58, 323-332. https://doi.org/10.1111/j.1574-6941.2006.00180.x,35,

275 2006.

Deutsch C., Sarmiento, J.L., Sigman, D.M., Gruber, N. and Dunne, J.P.: Spatial coupling of nitrogen inputs and losses in the ocean, Nature, 445, 163-167. https://doi.org/10.1038/nature05392, 2007.

Duce, R. A., LaRoche, J., Altieri, K., Arrigo, K. R., Baker, A. R., Capone, D. G., Cornell, P.S., Dentener, F. Galloway, J., Ganeshram, R. S. Geider, R.J., Jickells,T. Kuypers, M.M. Langlois, R., Liss, P.S., Liu, S. M., Middelburg, J. J., Moore, C.M., Nickovic, S. Oschlies, A.,

280 Pedersen, T., Prospero, J., Schlitzer, R., Seitzinger, S., Sorensen, L.L., Uematsu, M. Ulloa, O, Voss, M., Ward, B. and Zamora, L.: Impacts of atmospheric anthropogenic nitrogen on the open ocean, Science, 320(5878), 893-897. https://doi.org/10.1126/science.1150369, 2008.

Falcón, L.I., Pluvinage S. and Carpenter, E.J,: Growth kinetics of marine unicellular N_2-fixing cyanobacterial isolates in continuous culture in relation to phosphorus and temperature, Marine Ecology Progress Series, 285, 3-9. https://doi.org/10.3354/meps285003, 2005.

Fennel, K., Losch, M., Schröter, J., and Wenzel, M.: Testing a marine ecosystem model: sensitivity analysis and parameter optimization, J.

285 Marine Syst., 28, 45-63. https://doi.org/10.1016/S0924-7963(00)00083-X, 2001.

Garcia, H. E., Locarnini, R. A., Boyer, T. P., Antonov, and Levitus, S.: World Ocean Database 2005, Volume 4: Nutrients (phosphate, nitrate, silicate) (NESDIS 4,, pp. 396) NOAA Atlas, U.S. Government Printing Office, Washington, D.C., 2006.

Getzlaff, J. and Dietze, H.: Effects of increased isopycnal diffusivity mimicking the unresolved equatorial intermediate current system in an earth system climate model. Geophys. Res. Letters, 40(10), 2166-2170. https://doi.org/10.1002/grl.50419, 2013.

290 Großkopf, T., Mohr, W., Baustian, T., Schunck, H., Gill, D., Kuypers, M. M. M.,Lavik, G., Schmitz, R.A., Wallace, D.W. R. and LaRoche, J.: Doubling of marine dinitrogen-fixation rates based on direct measurements. Nature, 488, 361-364. https://doi.org/10.1038/nature11338, 2012.

Gruber, N.: The Dynamics of the Marine Nitrogen Cycle and its Influence on Atmospheric CO_2 Variations. In M. Follows and T. Oguz (Eds.) The Ocean Carbon Cycle and Climate. NATO Science Series (Series IV: Earth and Environmental Sciences) (Vol. 40, pp. 97-148).

295 Springer, Dordrecht. https://doi.org/10.1007/978-1-4020-2087-2_4, 2004.

Gruber, N.: Elusive marine nitrogen fixation, Proc. Natl. Acad. Sci. U.S.A., 113(16), 4246-4248. https://doi.org/10.1073/pnas.1603646113, 2016.

Gruber, N., and Sarmiento, J. L.: Global patterns of marine nitrogen fixation and denitrification. Global Biogeochem. Cycles, 11(2), 235-266. https://doi.org/10.1029/97GB00077, 1997.

300 Hawser, S.P., O'Neil, J.M., Roman, M.R. and Codd, G.A.: Toxicity of blooms of the cyanobacterium-trichodesmium to zooplankton. J. Appl. Phycol., 4, 79-86. https://doi.org/10.1007/BF00003963, 1992.

Kemena, T. P. , Oschlies, A. , Wallmann, K. J. G. , Landolfi, A. and Dale, A. W.: Ocean phosphorus inventory: large uncertainties in future projections on millennial timescales and their consequences for ocean deoxygenation. Earth System Dynamics, 10 (3), 539-553. https://doi.org/110.5194/esd-10-539-2019, 2019.

305 Keller, D. P., Oschlies, A., and Eby, M.: A new marine ecosystem model for the University of Victoria Earth System Climate Model, Geosci. Model Dev., 5, 1195–1220, https://doi.org/10.5194/gmd-5-1195-2012, 2012.

Keller, D. P., Feng, E. Y., and Oschlies, A.: Potential climate engineering effectiveness and side effects during a high carbon dioxide-emission scenario. Nature communications, 5. https://doi.org/10.1038/ncomms4304, 2014

Krishnamurthy, A., Moore, J. K, Zender,, C.S. and Luo, C.: Effects of atmospheric inorganic nitrogen deposition on ocean biogeochemistry,
310 J. Geophys. Res., 112, G02019. https://doi.org/10.1029/2006JG000334, 2007.

Krishnamurthy, A., Moore, J.K., Mahowald, N., Luo, C., Doney, S.C., Lindsay, K and Zender, C.S.: Impacts of increasing anthropogenic soluble iron and nitrogen deposition on ocean biogeochemistry, Global Biogeochem. Cycles, 23, GB3016. https://doi.org/1 0.1029/2008GB003440, 2009.

Landolfi, A. , Dietze, H., Koeve, W. and Oschlies, A.: Overlooked runaway feedback in the marine nitrogen cycle: the vicious cycle. Biogeo-
315 sciences (BG), 10, 1351-1363. https://doi.org/10.5194/bg-10-1351-2013, 2013.

Landolfi, A., Koeve, W., Dietze, H., Kähler, P., and Oschlies, A.: A new perspective on environmental controls of marine nitrogen fixation.Geophysical Res. Letters, 42(11), 4482-4489. https://doi.org/10.1002/2015GL063756, 2015.

Landolfi, A., Somes, C. J., Koeve, W., Zamora, L. M., and Oschlies, A.: Oceanic nitrogen cycling and N_2O flux perturbations in the Anthropocene. Global Biogeochem. Cycles, 31(8), 1236-1255. https://doi.org/10.1002/2017GB005633, 2017.

320 Landolfi, A., Kähler, P., Koeve, W., and Oschlies, A.: Global marine N_2 fixation estimates: From observations to models. Frontiers in Microbiology, 9. https://doi.org/10.3389/fmicb.2018.02112, 2018.

LaRoche, J., and Breitbarth , E.: Importance of the diazotrophs as a source of new nitrogen in the ocean, J. Sea Res., 53, 67-91. https://doi.org/10.1016/j.seares.2004.05.005, 2005.

Large, W. G., Danabasoglu, G., McWilliams, J. C., Gent, P. R., and Bryan, F. O.: Equatorial circulation of a global
325 ocean climate model with anisotropic horizontal viscosity, J. Phys. Oceanogr., 31, 518-536. https://doi.org/10.1175/1520-0485(2001)031<0518:ECOAGO>2.0.CO;2, 2001.

Löptien, U. and Dietze, H.: Constraining parameters in marine pelagic ecosystem models – is it actually feasible with typical observations of standing stocks? Ocean Science, 11 (4), 573-590, https://doi.org/10.5194/os-11-573-2015, 2015.

Löptien, U. and Dietze, H.: Effects of parameter indeterminacy in pelagic biogeochemical modules of Earth System Models on projections
330 into a warming future: The scale of the problem. Global Biogeochem. Cycles, 31 (7), 1155-1172. https://doi.org/10.1002/2017GB005690, 2017.

Löptien, U., and Dietze, H.: Reciprocal bias compensation and ensuing uncertainties in model-based climate projections: pelagic biogeochemistry versus ocean mixing. Biogeosciences (BG), 16(9), 1865-1881. https://doi.org/10.5194/bg-16-1865-2019, 2019.

Luo, Y. W., Doney, S. C., Anderson, L. A., Benavides, M., Berman-Frank, I., Bode, A., Bonnet, S. Boström, K.H. Böttjer, D., Capone,
335 D.G., Carpenter, E.J., Chen, Y.L., Church, M.J., Dore, J.E., Falcón, L.I., Fernández, A., Foster,R.A., Furuya, K. Gómez, F. Gundersen, K., Hynes, A.M. Karl, D.M., Kitajima, S. Langlois, R.J., LaRoche, J., Letelier, R.M., Maranon, E., McGillicuddy Jr., D.J., Moisander, P.H., Moore, C.M., Mourino-Carballido, B., Mulholland, M.R., Needoba, J.A., Orcutt, K.M., Poulton, A.J., Rahav, E., Raimbault, P., Rees, A.P., Riemann, L., Shiozaki,, T. Subramaniam, A., Tyrrell, T. Turk-Kubo, K.A., Varela, M., Villareal, T.A., Webb, E.A., White, A.E., Wu,

J. and Zehr, J.P.: Database of Diazotrophs in Global Ocean: Abundance, Biomass, and Nitrogen Fixation Rates. Earth System Science
340   Data, 4(1), 47-73. https://doi.org/10.5194/essd-4-47-2012, 2012.

Luo, Y. W., Doney, S. C., Anderson, L. A., Benavides, M., Berman-Frank, I., Bode, A., Bonnet, S. Boström, K.H. Böttjer, D., Capone,
         D.G., Carpenter, E.J., Chen, Y.L., Church, M.J., Dore, J.E., Falcón, L.I., Fernández, A., Foster,R.A., Furuya, K. Gómez, F. Gundersen, K.,
         Hynes, A.M. Karl, D.M., Kitajima, S. Langlois, R.J., LaRoche, J., Letelier, R.M., Maranon, E., McGillicuddy Jr., D.J., Moisander, P.H.,
         Moore, C.M., Mourino-Carballido, B., Mulholland, M.R., Needoba, J.A., Orcutt, K.M., Poulton, A.J., Rahav, E., Raimbault, P., Rees, A.P.,
345   Riemann, L., Shiozaki,, T. Subramaniam, A., Tyrrell, T. Turk-Kubo, K.A., Varela, M., Villareal, T.A., Webb, E.A., White, A.E., Wu, J.
         and Zehr, J.P.: Global distributions of diazotrophs abundance, biomass and nitrogen fixation rates - Gridded data product (NetCDF) - Con-
         tribution to the MAREDAT World Ocean Atlas of Plankton Functional Types. PANGAEA, https://doi.org/10.1594/PANGAEA.774851,
         2012.

McMahon, K. W., M. D. McCarthy, O. A. Sherwood, T. Larsen, and T. P. Guilderson: Millennial-scale plankton regime shifts in the subtrop-
350   ical North Pacific Ocean, Science, 350, 1530-1533. https://doi.org/10.1126/science.aad6946, 2015.

Mengis, N. , Martin, T. , Keller, D. P. and Oschlies, A.: Assessing climate impacts and risks of ocean albedo modification in the Arctic.
         Journal of Geophysical Research: Oceans, 121 (5), 3044-3057. DOI 10.1002/2015JC011433, 2016.

Mills, M.M. and Arrigo, K.R.: Magnitude of oceanic nitrogen fixation influenced by the nutrient uptake ratio of phytoplankton. Nature
         Geosci., 3, 412-416. https://doi.org/10.1038/ngeo856, 2010.

355   Moore, J. K., Doney, S. C., Kleypas, J. A., Glover, D. M., and Fung, I. Y. : An intermediate complexity marine ecosystem model for the
         global domain. Deep Sea Res. Part II: Topical Studies in Oceanography, 49(1-3), 403-462. https://doi.org/10.1016/S0967-0645(01)00108-
         4, 2001.

Mulholland, M. R., Floge, S., Carpenter, E. J.,and Capone, D. G.: Phosphorus dynamics in cultures and natural populations of Trichodesmium
         spp. Marine Ecology Progress Series, 239, 45-55. https://doi.org/10.3354/meps239045, 2002.

360   Oschlies, A., Pahlow, M., Yool, A., and Matear, R. M.: Climate engineering by artificial ocean upwelling: channelling the sorcerer's appren-
         tice, Geophysical Res. Letters, 37, 1-5. https://doi.org/10.1029/2009GL041961, 2010.

Pacanowski, R.C.: MOM 2 documentation, user's guide and reference manual. GFDL Ocean Group Tech. Rep, 3(3), 232, 1995.

Pahlow, M., Dietze, H. and Oschlies, A.: Optimality-based model of phytoplankton growth and diazotrophy. Marine Ecology Progress Series,
         489, 1-16. https://doi.org/10.3354/meps10449, 2003.

365   Paulsen, H., Ilyina, T., Six, K. D., and Stemmler, I. : Incorporating a prognostic representation of marine nitrogen fixers into the global ocean
         biogeochemical model HAMOCC. J. Advances in Modeling Earth Systems, 9(1), 438-464. https://doi.org/10.1002/2016MS000737, 2017.

Polovina, J. J., Howell, E. A., and Abecassis, M.: Ocean's least productive waters are expanding. Geophysical Research Letters, 35(3),
         L03618. https://doi.org/10.1029/2007GL031745, 2008.

Pontius, R.G,, Thontteh, O. and Chen, H.: Components of information for multiple resolution comparison between maps that share a real
370   variable. Environmental and Ecological Statistics, 15 (2), 111-142, https://doi.org/10.1007/s10651-007-0043-y, 2008.

Reith, F., Keller, D. P. and Oschlies, A. (2016). Revisiting ocean carbon sequestration by direct injection: A global carbon budget perspective,
         Earth System Dynamics, 7, 797-812. https://doi.org/10.5194/esd-7-797-2016

Riahi, K., Rao, S., Krey, V., Cho, C., Chirkov, V., Fischer, G., Kindermann, G., Nakicenovic, N. and Rafaj, P.: RCP 8.5- A scenario of
         comparatively high greenhouse gas emissions. Climatic Change, 109(1-2), 33. https://doi.org/10.1007/s10584-011-0149-y, 2011.

375   Sauerland, V., Löptien, U. , Leonhard, C., Oschlies, A. and Srivastav, A.: Error assessment of biogeochemical models by lower bound
         methods (NOMMA-1.0). Geoscientific Model Development, 11 (3). 1181-1198, https://doi.org/ 10.5194/gmd-2017-133, 2018.

Biogeosciences
Discussions
Open Access
EGU

Schmittner, A., Oschlies, A., Matthews, H. D., and Galbraith, E. D.: Future changes in climate, ocean circulation, ecosystems, and biogeo-chemical cycling simulated for a business-as-usual CO_2 emission scenario until year 4000 AD, Global Biogeochem. Cycles, 22, GB1013. https://doi.org/10.1029/2007GB002953, 2008.

380 Somes, C. J., and Oschlies, A.: On the influence of "non-Redfield" dissolved organic nutrient dynamics on the spatial distri-bution of N2 fixation and the size of the marine fixed nitrogen inventory. Global Biogeochemical Cycles, 29(7), 973-993, https://doi.org/10.1002/2014GB005050, 2015.

Somes, C. J., Schmittner, A., Galbraith, E. D., Lehmann, M. F., Altabet, M. A., Montoya, J. P., Letelier, R. M., Mix, A. C., Bourbon-nais, A., and Eby, M.: Simulating the global distribution of nitrogen isotopes in the ocean, Global Biogeochem. Cycles, 24, GB4019.

385 https://doi.org/10.1029/2009GB003767, 2010.

Tang, W., Wang, S., Fonseca-Batista, D., Dehairs, F., Gifford, S., Gonzalez, A. G., Gallinari, M., Planquette, H., Sarthou, G. and Cassar, N.: Revisiting the distribution of oceanic N_2 fixation and estimating diazotrophic contribution to marine production. Nature communications, 10(1), 831. https://doi.org/10.1038/s41467-019-08640-0, 2019.

Tang, W., Li, Z., and Cassar, N.: Machine Learning Estimates of Global Marine Nitrogen Fixation. Journal of Geophysical Research: Bio-

390 geosciences, 124(3), 717-730, https://doi.org/10.1029/2018JG004828, 2019.

Vahtera, E., Conley, D.J., Gustafsson, B.G., Kuosa, H., Pitknen, H., Savchuk, O.P. and Wulf, F.: Internal ecosystem feedbacks enhance nitrogen-fixing cyanobacteria blooms and complicate management in the Baltic Sea. AMBIO: A journal of the Human Environment, 36(2), 186-194. https://doi.org/10.1579/0044-7447(2007)36[186:IEFENC]2.0.CO;2, 2007.

Wang, W. L., Moore, J. K., Martiny, A. C., and Primeau, F. W.: Convergent estimates of marine nitrogen fixation. Nature, 566(7743), 205-211.

395 https://doi.org/10.1038/s41586-019-0911-2, 2019.

Wasmund, N.., Voss, M. and Lochte, K.: Evidence of nitrogen fixation by non-heterocystous cyanobacteria in the Baltic Sea and re-calculation of a budget of nitrogen fixation. Mar. Ecol. Prog. Ser., 214, 1-14. https://doi.org/10.3354/meps214001, 2001.

Weaver, A. J., Eby, M., Wiebe, E. C., Bitz, C. M., Duffy, P. B., Ewen, T. L., Fanning , A.F., Holland, M.M., MacFadyen, A., Matthews, H.D., Meissner, K. J., Saenko, O., Schmittner, A., Wang, H. and Yoshimori, M.: The UVic Earth System Climate

400 Model: Model description, climatology, and applications to past, present and future climates. Atmosphere-Ocean, 39(4), 361-428. https://doi.org/10.1080/07055900.2001.9649686, 2001.

Willmott, C.J. and Matsuura, K.: Advantages of the mean absolute error (MAE) over the root mean square error (RMSE) in assessing average model performance. Climate Research, 30, 79-82, https://doi.org/10.3354/cr030079, 2005.

Table 1. Relevant model parameters in the reference model version REF and the setups GRAZ and OLIGO. Bold values refer to parameters obtained during tuning exercises. Note that θ_o has been calculated with the equation $\theta_d + \theta_o = 0.4$. The last column gives the ranges, in which the parameters are varied to minimize the misfit to the estimate by Wang et al. (2019).

Param.	Description	Units	Ref. Value	GRAZ	OLIGO	Range
C_d	Growth handycap of diazotrophs	unitless	**0.3**	0.4	0.4	0.3-0.6
k_P^d	Half-saturation constant for PO$_4$-limitation for diazotrophs	mmol PO$_4$/m^3	0.044	0.044	**0.009**	0.002-0.044
θ_d	Grazing preference for diazotrophs	unitless	0.1	**0.14**	**0.2**	0.08-0.2
θ_o	Grazing preference for phytoplankton	unitless	0.3	**0.26**	**0.2**	0.2-0.32
J_O^{max}	Maximum potential growth rate of phytoplankton at $0°C$	day^{-1}	0.6	0.6	0.6	-
J_D^{max}	Maximum potential growth rate of diazotrophs at $0°C$	day^{-1}	0.6	0.6	0.6	-
k_{Fe}	Half-saturation constant for iron (Fe)-limitation	mmol Fe/m^3	0.1	0.1	0.1	-
k_N	Half-saturation constant for NO$_3$-limitation for phytoplankton	mmol NO$_3$/m^3	0.7	0.7	0.7	-
k_P	Half-saturation constant for PO$_4$-limitation for phytoplankton	mmol PO$_4$/m^3	0.044	0.044	0.044	-
α	Initial slope of the P-I-curve	(W/m^2)$^{-1}$d^{-1}	0.1	0.1	0.1	-
T_b	E-folding temperature of biological rates	$°C$	5.65	5.65	5.65	-

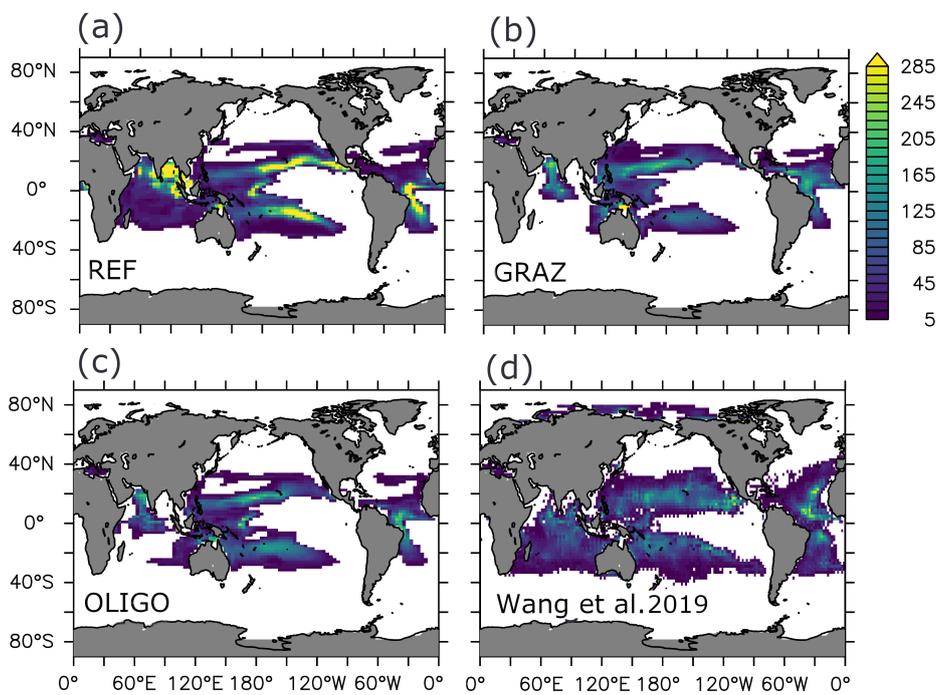**Figure 1.** Simulated nitrogen fixation in $mmol\ N/m^2/yr$ for (a) the reference model, (b) the simulations based on OLIGO, (c) GRAZ and (d) estimate by Wang et al. (2019).
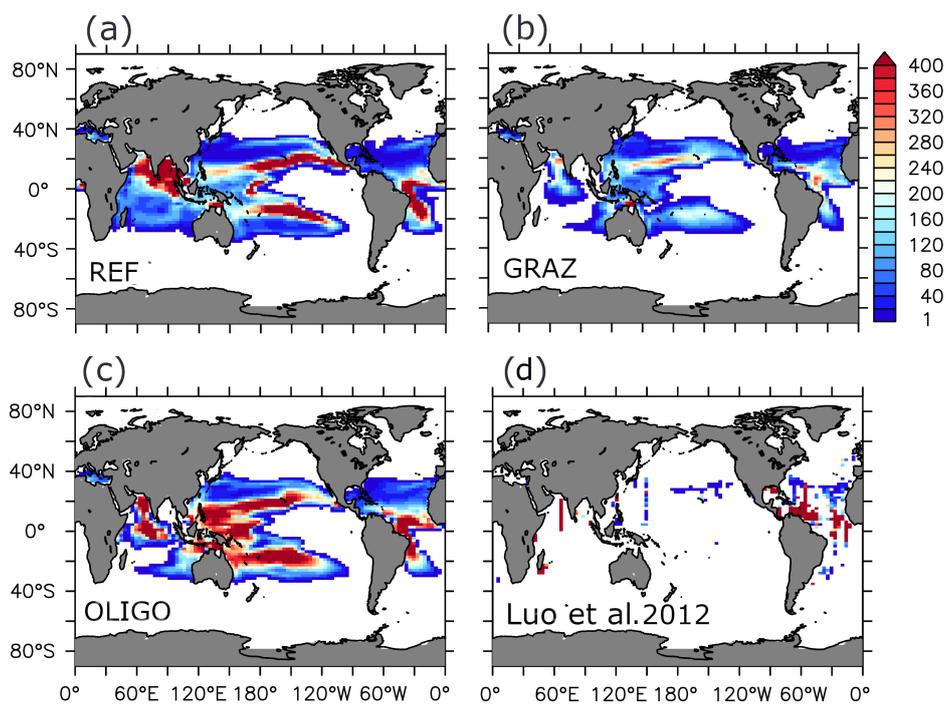
Figure 2. Annual mean non-zero diazotrophic biomass integrated over the upper 100m in $mg\ C/m^2$: (a) for the reference model, (b) the simulations based on OLIGO, (c) GRAZ and (d) as observed (Luo et al., 2012). The observations were interpolated linearly over depth and then gridded onto the model grid.
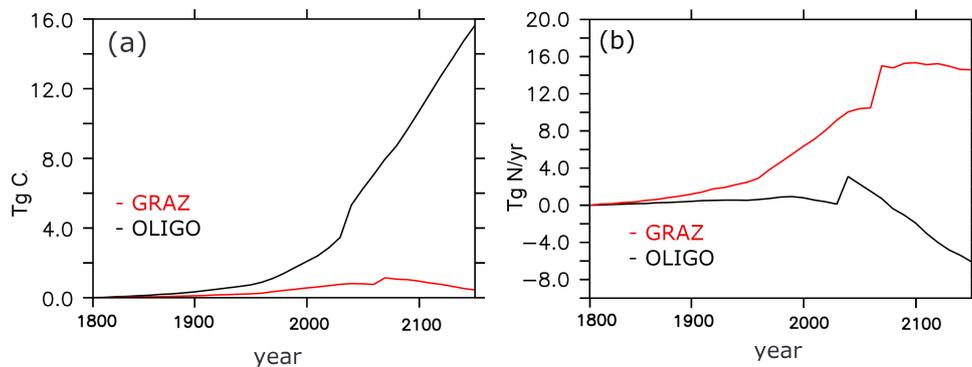

Figure 3. Anomalous projected evolution of (a) global annual mean biomass of diazotrophic biomass in units $Tg\ C$ and (b) global annual mean nitrogen fixation in units $Tg\ N\ yr^{-1}$.